Optik - International Journal for Light and Electron Optics 181 (2019) 1113–1121

Contents lists available at ScienceDirect

Optik

journal homepage: www.elsevier.com/locate/ijleo

Original research article

Blue emitting Ce^{3+}-doped $CaYAl_3O_7$ phosphors prepared by combustion route

Yong-Keun Choi[a], Pramod Halappa[b], C. Shivakumara[b], Vikas Dubey[c], Vijay Singh[d,*]

[a] Department of Biological Engineering, Konkuk University, Seoul 05029, Republic of Korea
[b] Solid State and Structural Chemistry Unit, Indian Institute of Science, Bangalore 560 012, India
[c] Department of Physics, Bhilai Institute of Technology, Raipur, Kendri, 493661, India
[d] Department of Chemical Engineering, Konkuk University, Seoul, 05029, Republic of Korea

ARTICLE INFO

Keywords:
Phosphor
Ce^{3+}
$CaYAl_3O_7$
Combustion

ABSTRACT

The solution-combustion route was used to synthesize series of Ce^{3+}-ion-activated $CaYAl_3O_7$ (CYO) blue-light-emitting phosphors. Formation of the tetragonal CYO structure was confirmed by the powder X-ray diffraction (XRD) studies. On substitution of Ce^{3+} ion to Ca site in $CaYAl_3O_7$ system, the photoluminescence spectra recorded at ultraviolet-light (360 nm) excitation. Photoluminescence excitation spectra at 360 nm showed the characteristic emission at 434 nm of the Ce^{3+} ion caused by 5d → 4f transitions. Increase in intensity can be seen up to 1 mol % of Ce^{3+} followed by quenching due to dipole-dipole interaction. The Commission Internationale de l'Eclairage (CIE - 1931) coordinates x = 0.1484 and y = 0.0987 of this phosphor are in the violet–blue region. The blue-color purity was found to be maximum 90% for 1 mol% Ce^{3+}-doped phosphor. The obtained CIE, CCT, and color-purity results illustrate the potentiality of Ce^{3+}-activated CYO phosphor for household-lighting and display-device applications.

1. Introduction

Nowadays, white light-emitting diodes (WLEDs) have gained much importance due to its admirable features including very high energy efficiency, compactness, easy for installation, long lifespan, low maintenance requirements, with vast design capabilities in terms of color creation and atmospheric mood lighting. Because of which WLEDs are hailed as the next-generation solid-state lighting [1,2]. The currently available WLEDs in the market produce white light by combining the blue light from light-emitting diode (LED) chips with the yellow emission from the yttrium aluminum garnet (YAG):cerium (Ce) phosphor. This kind of combination gives a poor color-rendering index (< 80) and a high color correlated temperature (CCT) because of the lack of a red-light component (more than 600 nm) and which is limiting its acceptance in practical application for prospective household and commercial applications.

One efficient way to generate white light is to combine a near-ultraviolet (NUV) indium gallium nitride (InGaN) chip (380–410 nm) with blue, green, and red phosphors which will yield a high color-rendering index and an effective color reproducibility [3–5]. To accomplish this goal, there is a necessity to discover a novel, efficient, high-color-purity, low-CCT and, broad-band blue-light-emitting phosphor in order to advance the color rendering index (CRI) value (> 85) for the attainment of a warm or natural white light. Typically, the broad emission bands exhibited from rare earth (RE)-ion-activated oxide phosphors are found in the blue, green, or red spectral regions under ultraviolet (UV)- or visible-wavelength excitations. Therefore, the contemporary solution of this issue involves an increasing attention toward the fabrication of low-thermal-quenching trichromatic (blue, green, and

* Corresponding author.
E-mail address: vijayjiin2006@yahoo.com (V. Singh).

https://doi.org/10.1016/j.ijleo.2018.10.213
Received 28 September 2018; Accepted 31 October 2018

red) phosphors of a high efficiency and a high chemical stability that can be excited by NUV LEDs [6].

Consequently, a new matrix and system of RE-doped WLED phosphors are being studied currently at a great extent. The general chemical formula of $CaYAl_3O_7$ is ABC_3O_7 (A = Ca, Sr and Ba; B = La, Gd and Y; C = Al or Ga), which belongs to the large families of the melilite structure [7]. Due to their structural features, Melilite compounds have been widely investigated as important optical materials. For instance, Singh et al. [8] highlighted the synthesis, characterization, and photoluminescence (PL) of Eu^{3+}–Ce^{3+} co-doped $CaLaAl_3O_7$ phosphors. Zhang et al. [9] revealed the luminescence properties of $SrGdGa_3O_7:RE^{3+}$ (RE = trivalent europium [Eu^{3+}], trivalent terbium [Tb^{3+}]) phosphors along with the energy transfer from the Gd^{3+} to the RE^{3+}. The potential red-emitting phosphor $CaSrAl_2SiO_7:Eu^{3+}$ for NUV LEDs has been reported by Jiao and Wang [10]. In addition, Zhang et al. [11] studied the blue-light emission from stress-activated $CaYAl_3O_7:Eu^{2+}$ as well as investigated the electro-mechano-optical luminescence from $CaYAl_3O_7:Ce^{3+}$ [12]. Number of investigations on RE-doped melilite families have been performed and can be found in the literature. These studies implied that the RE-doped melilite crystal is an interesting laser host material owing to its broadened absorption and emission spectra that are useful for diode laser pumping and a tunable laser generation, respectively [13]. $CaYAl_3O_7$ host materials have attracted much attention because of the great advantages as it possess qualities like robust stability, cheap raw materials, simple synthesis conditions, and sound luminescence properties [14–16].

An economical preparation procedure that can provide a highly luminescent phosphor with excellent radiative properties, requires an appropriate synthesis technique. Several wet chemical methods such as conventional solid state method, sol–gel process, micro-emulsion method, co-precipitation reaction, surfactant-assisted hydrothermal approach, spray drying, freeze drying, combustion synthesis, electrochemical method and so on can be used to prepare these phosphor materials but some of them are having drawbacks like requirement of high temperatures, long durations, and costly, while sophisticated instrumentation might also be needed to perform the experiment. Among them, the urea (NH_2CONH_2)-catalyzed combustion method finds many advantages such as low heating temperatures, short durations and high product-purity values. It is a facile process, with homogeneous mass-scale synthesis of high-quality phosphors along with an excellent redispersibility, a more effective luminescence yield, low costs and abundant precursors thereby making this method cost-effective. In this combustion synthesis, the NH_2CONH_2 is used as the reductant/fuel and nitrate is used as the oxidant. This process is composed of the formation of a stable metal complex with NH_2CONH_2. In addition, the reaction will be self-propogatory upon heating and will combust to yield a homogeneous product [17].

In the present work, Ce^{3+}-doped $CaYAl_3O_7$ phosphor is prepared using the combustion synthesis and investigated as a new violet–blue phosphor. To the best of authors' knowledge, a detailed spectroscopic investigation of $CaYAl_3O_7:Ln^{3+}$ (Ln = Ce) under a UV excitation has not been previously reported in the literature [14–16]; considering this fact, the aim of the present research work is to estimate different spectral parameters. For different Ce^{3+} concentrations, parameters like the color-purity and correlated color temperature (CCT) values were calculated. Subsequently, Ce^{3+} host matrix has been proposed as a suitable blue-emitting phosphor for white-light emissions in industrial applications.

2. Experimental

A series of Ce^{3+}-activated $CaYAl_3O_7$ phosphors with the varied Ce^{3+} concentrations of 0.5, 1, 3, 5, 7 and 9 mol% were synthesized by the solution-combustion method and are denoted as CY1, CY2, CY3, CY4, CY5 and CY6, respectively, The synthesis is based on the exothermic reaction between the fuel and the oxidizer. For the completion of the combustion, the oxidizer-to-fuel (O/F) ratio was calculated by maintaining O/F = 1 [8]. The stoichiometric amounts of the constituent raw materials such as calcium nitrate tetrahydrate ($Ca[NO_3]_2{\cdot}4H_2O$), yttrium nitrate hexahydrate ($Y[NO_3]_3{\cdot}6H_2O$), aluminium nitrate nonahydrate ($Al[NO_3]_3{\cdot}9H_2O$), cerium nitrate hexahydrate ($Ce[NO_3]_3{\cdot}6H_2O$), and urea (NH_2CONH_2) were weighed and dissolved in a minimum amount of distilled water in a 100-ml china dish to obtain a homogeneous solution. Then, the solution was transferred to a muffle furnace that had been maintained at 550 ± 10 °C. The solution underwent a dehydration that was followed by decomposition with the evolution of gases such as nitrogen (N_2) and carbon dioxide (CO_2). The mixture then frothed and swelled, forming foam that ruptured with a flame upon the ignition of the combustible gases, and it subsequently glowed to incandescence. The whole process was completed within 5 min. After the combustion process, the resultant voluminous foamy powder was gently ground using a mortar and pestle and was then used for further characterization. The details of the sample codes and the starting materials along with required weights are given in Table 1.

Table 1
Detailed information of sample codes and weight of required starting materials.

Sample code	Cerium (mol %)	Weight of starting materials (g)				
		$Ca(NO_3)_2{\cdot}4H_2O$	$Ce(NO_3)_3{\cdot}6H_2O$	$Y(NO_3)_3{\cdot}6H_2O$	$Al(NO_3)_3{\cdot}9H_2O$	Urea
CY1	0.5	0.3481	0.0032	0.5672	1.6666	1.0437
CY2	1	0.3463	0.0064	0.5672	1.6666	1.0437
CY3	3	0.3393	0.0192	0.5672	1.6666	1.0437
CY4	5	0.3323	0.0320	0.5672	1.6666	1.0437
CY5	7	0.3253	0.0448	0.5672	1.6666	1.0437
CY6	9	0.3183	0.0576	0.5672	1.6666	1.0437

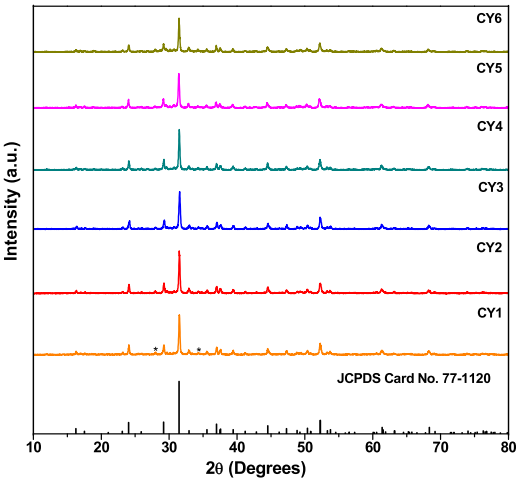

Fig. 1. Powder XRD pattern of as-prepared $CaYAl_3O_7:Ce^{3+}$ (CY1 to CY6) phosphor (* indicates unknown impurity).

The X-ray diffraction (XRD) patterns of the as-prepared samples were recorded using the Miniflex-II diffractometer (Rigaku, Japan) that was operated in the Bragg–Brentano focusing geometry at 40 kV and 30 mA, while Cu-Kα radiation (λ = 1.5406 Å) served as the X-ray source. The XRD patterns were taken with the scan rate of 5°/min in the 2θ range of 10–80°. The morphological investigations were conducted using the S-3400 scanning electron microscope (SEM) apparatus (Hitachi, Japan). The PL emission and excitation spectra of the samples were recorded using the RF-5301PC spectrofluorophotometer (Shimadzu, Japan) equipped with a xenon lamp. All of the measurements were performed at room temperature and under an ambient condition.

3. Results and discussion

3.1. X-ray diffraction studies

Powder XRD has been done in the 2θ range of 10–80°. Fig. 1 illustrates patterns of the as-prepared Ce^{3+}-activated $CaYAl_3O_7$ phosphors. The diffraction peaks were matched with tetragonal phase of $CaYAl_3O_7$ (JCPDS Card No. 77-1120) of powder-diffraction standards. Crystallite size was calculated for the main XRD peak by well-known Scherrer's equation $D = 0.9\,\lambda/\beta\cos\theta$, where λ is the wavelength of the incident X-ray, θ is the corresponding Bragg's diffraction angle, and β is the full width at half maximum (FWHM) of the main (211) peak. Table 2 explores the FWHM and the crystallite sizes of all the samples. From this table, it can be seen that crystallite sizes are in the range of 36–43 nm. The XRD analysis showed that the combustion-synthesis method is useful for the preparation of the tetragonal $CaYAl_3O_7$ structure, even at furnace temperatures as low as 550 °C and in a shorter duration of few minutes.

3.2. Scanning electron microscopy

Fig. 2 shows the SEM images of the $CaYAl_3O_7$:Ce (CY2) phosphors. From Fig. 2 (A) and 2 (B) the irregular shaped agglomerated particles can be seen. Fig. 2 (C) is the magnified view of Fig. 2 (B), wherein Zone (b) with magnification power of 2200 × . Likewise, Fig. 2 (D) shows a magnified view of Fig. 2 (C), wherein Zone (c) is shown at magnification of 4000 × . From these high-magnification images pores, voids, and cracks in the particles are visible. The evolution of large amounts of gases during the combustion process has caused the formation of pores and cracks in the material. Numerous nanoparticle aggregates are formed in the combustion product; this is the inherent nature of combustion synthesis.

Table 2
FWHM and crystallite size of as-prepared $CaYAl_3O_7:Ce^{3+}$ phosphor.

Sample code	FWHM (°)	Crystalline size (nm)
CY1	0.2037	42.33
CY2	0.2071	41.65
CY3	0.2384	36.18
CY4	0.2025	42.07
CY5	0.2133	40.43
CY6	0.2137	40.36

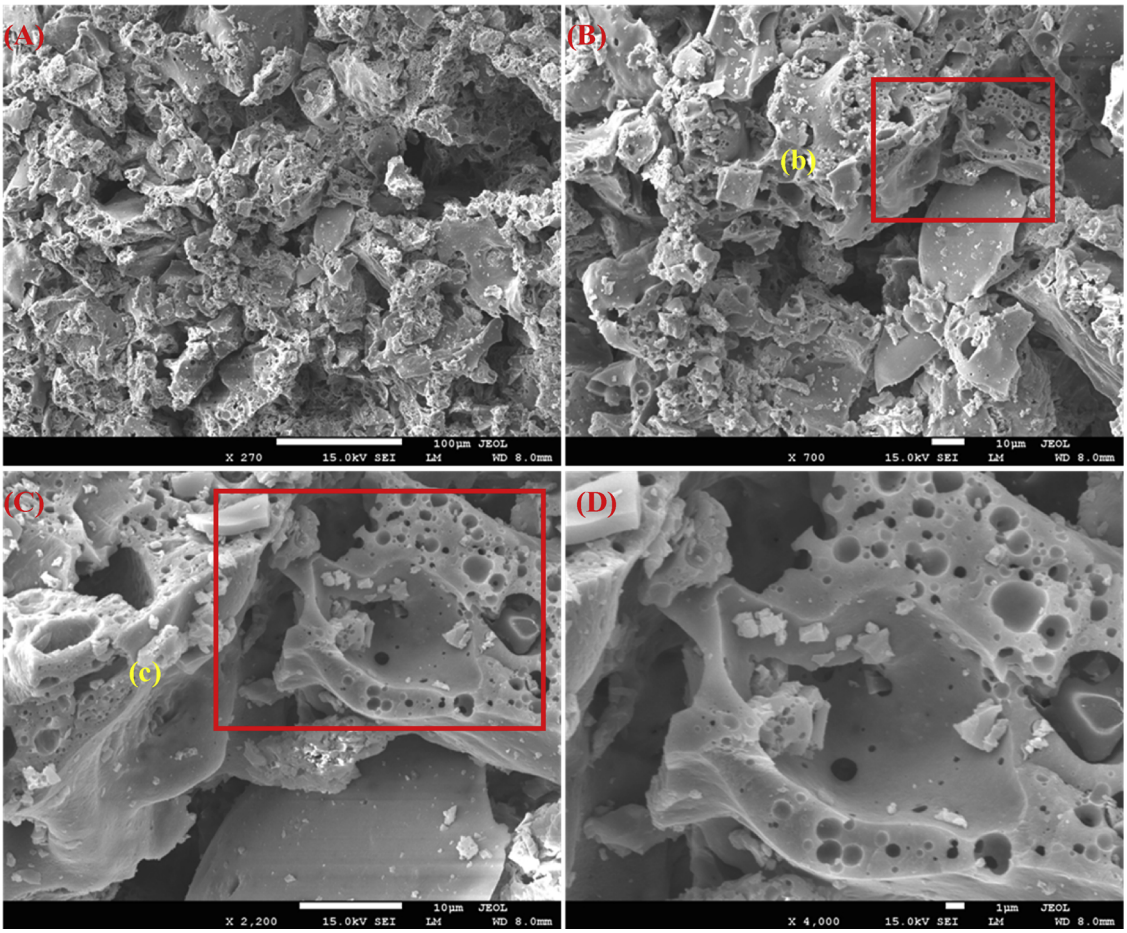

Fig. 2. Scanning electron micrographs of as-prepared $CaYAl_3O_7:Ce^{3+}$ (CY2) phosphor.

3.3. Photoluminescence analysis

Figs. 3(a) and 3(b), represents the PL-excitation spectrum (λem = 434 nm) and PL-emission spectrum (λex = 360 nm) of the as-prepared $CaYAl_3O_7:Ce^{3+}$ phosphors respectively. The excitation spectrum was monitored at 434 nm and exhibited a broad band at 360 nm that corresponds to the transition from the 4f state to the 5d state of the Ce^{3+}, which is very important for the excitation absorption of an NUV-LED chip. The broad emission peak observed at 434 nm under the 360-nm excitation is because of the

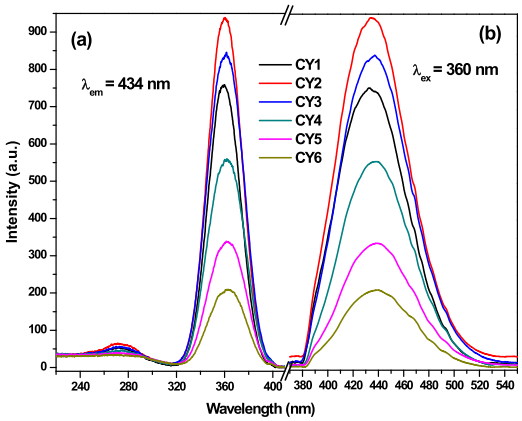

Fig. 3. Photoluminescence spectra of as-prepared $CaYAl_3O_7:Ce^{3+}$ (CY1 to CY6) phosphors: (a) excitation spectrum (λ_{em} = 434 nm) and (b) emission spectrum (λ_{ex} = 360 nm).

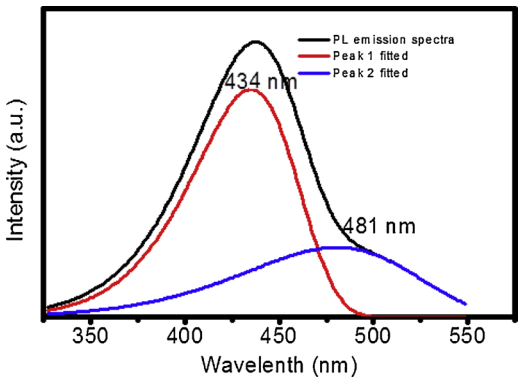

Fig. 4. Typical photoluminescence emission spectra fitted with Gaussian fit for $CaYAl_3O_7:Ce^{3+}$ (1 mol %, CY2) phosphor.

transitions from the lowest component of the 5d state to the $^2F_{5/2}$ and $^2F_{7/2}$ levels of the Ce^{3+}. In case of variable Ce^{3+} doping concentration (0.5–9 mol%) in the CYO host, the broad peak in the UV region (434 nm) is due to the 5d → 4f($^2F_{5/2}$) and 5d → 4f ($^2F_{7/2}$) transitions of the Ce^{3+} [18–20]. The 1 mol% is the optimized Ce^{3+} concentration for the CYO:Ce^{3+} phosphor, which may be applicable for the blue-light emission in display-device applications. For the composition of $CaYAl_3O_7:Ce^{3+}$ (1 mol%, CY2) phosphor, the emission band, however, can be decomposed into two clearly separated Gaussian components red and blue lines in Fig. 4 having maximum-intensity levels of 434 and 481 nm. Additionally, two possible causes of the emission bands for the Ce^{3+} ions in one specific lattice site can be explained as 1) the splitting of the transition from the lowest 5d excited state to the 4f ground states by the $^2F_{5/2}$ and $^2F_{7/2}$ spin–orbit, and 2) the presence of two different Ce^{3+}-associated luminescent centers on both the Ca^{2+} and Y^{3+} sites in CYO:Ce^{3+} [21–26]. There is possibility that Ce^{3+} might occupy both the Ca^{2+} and Y^{3+} sites as the radii of Ce^{3+} and Ca^{2+} are very close; but, as shown in Fig. 4, the shape of the PL-emission spectra monitored for 360 nm is almost the same as that of the fitted peak 1, suggesting that the occupation of Ce^{3+} on both the sites is incompetent. Thus, it has been further demonstrated that the Ce^{3+} only occupies the Y^{3+} crystal sites, as previously mentioned and this is a possible reason for showing two emission bands by the Ce^{3+} when it is fitted using the Gaussian fit [26].

3.4. Concentration quenching

With the increasing concentration of Ce^{3+}, the excitation and emission spectral intensities of the samples increased systematically {as shown respectively in Fig. 5 (a) and (b)} without any change of the peak positions up to 1 mol%. Fig. 6 depicts varying emission

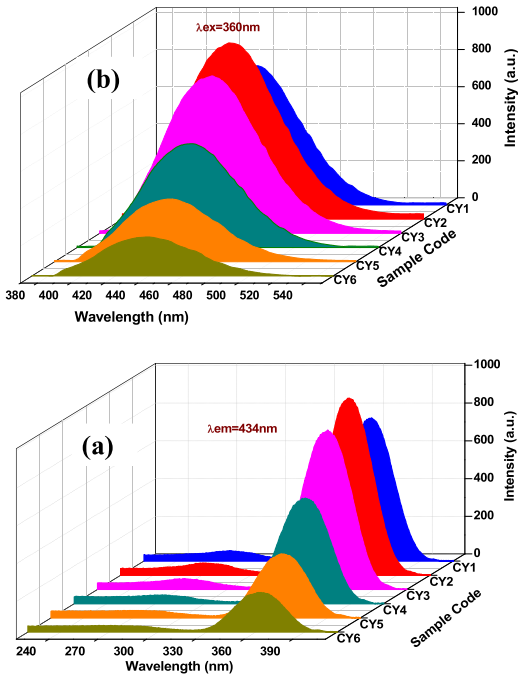

Fig. 5. PL plot in 3D (a) excitation and (b) emission spectra of $CaYAl_3O_7:Ce^{3+}$ (CY1-CY6) phosphors.

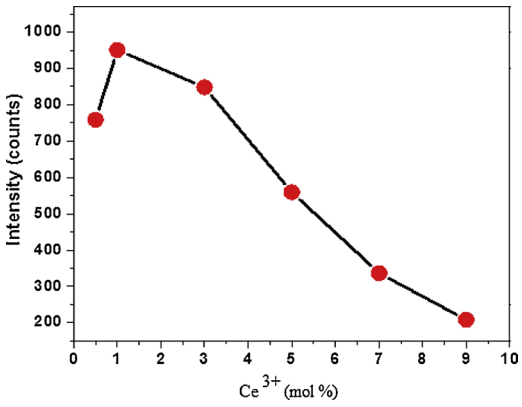

Fig. 6. Photoluminescence emission intensity as a function of Ce^{3+} ion concentrations in $CaYAl_3O_7:Ce^{3+}$ (CY1 to CY6).

intensity with respect to Ce^{3+} concentration and the concentration quenching taking place at 1 mol% of the Ce^{3+} concentration. This concentration quenching is correlated with the energy transfer from one of the Ce^{3+} ions to another Ce^{3+} ion either via the coupling of the phonon with the electron, or via a multipole interaction [27,28]. There are two possible mechanisms for energy transfer among the two Ce^{3+} ions and they are via an exchange interaction or a multipole–multipole interaction. The type of interaction can be identified by using Blasse formula after calculating the critical distance (R_c) between the two Ce^{3+} ions in the CYO host, as per the following [29]:

$$R_c \approx 2\left[\frac{3V}{4\pi x_c N}\right]^{1/3}, \tag{1}$$

where x_c represents the critical concentration of the Ce^{3+}, N is the number of cations in the unit cell, and V is the volume of the unit cell. In our case, the R_c is estimated to be 8.83 Å indicating quenching by the exchange interaction of the electric multipolar type interactions must occur in this case. Generally, multipolar interaction includes the dipole–quadrupole (d–q), dipole–dipole (d–d), and quadrupole–quadrupole (q–q) interactions [30]. And by using the Van Uitert equation, the interaction type that is involved in the energy transfer can be determined [31].

$$\frac{I}{x} = \frac{k}{(1+\beta(x)^{\theta/3})}, \tag{2}$$

where I/x is the emission intensity per activator (x), β and k are the constants for a given host lattice, and θ represents the interaction type between rare-earth ions; here, θ = 6, 8, and 10 correspond to the d–d, d–q, and q–q interactions, respectively. Fig. 7 shows a graph of the I/x versus x is on the logarithmic scale. The graph is of a linear type, having slope of -1.404 which results in a θ value of approximately 6, indicating that the d–d interaction type is the reason behind the concentration quenching in the $CaYAl_3O_7:Ce^{3+}$ phosphors.

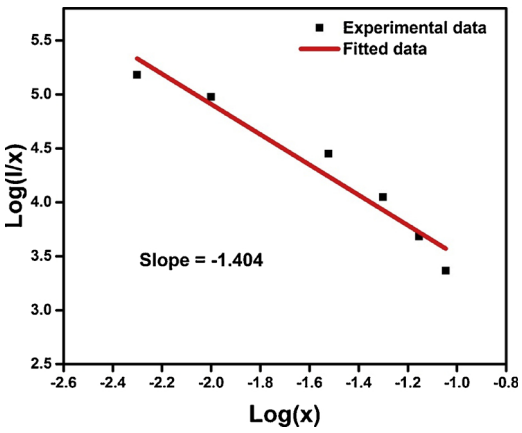

Fig. 7. log(I/x) versus log(x) plot of $CaYAl_3O_7:Ce^{3+}$ phosphors.

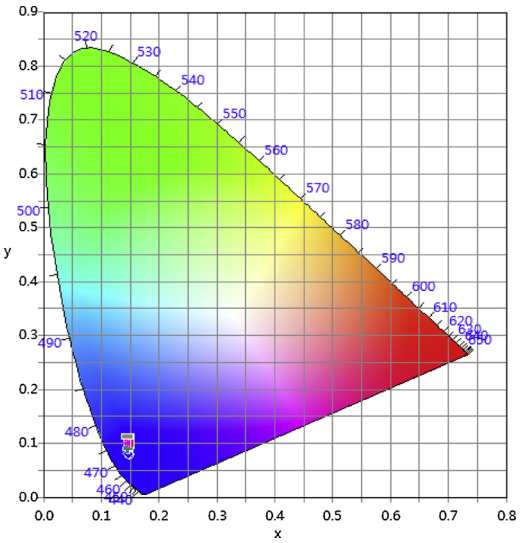

Fig. 8. CIE -1931 chromaticity diagram for $CaYAl_3O_7:Ce^{3+}$ (CY1–CY6) phosphors.

3.5. Color characteristics

To test the practical applications of these phosphors, the color quality was visualized in terms of the Commission International de l'Eclairage (CIE) 1931 chromaticity coordinates. These color coordinates distinguish the following three primary colors i. e. red, green, and blue for the human-eye system. So, the color of any light source can be represented on the (x, y) coordinates in this color space [32]. Fig. 8 shows the CIE coordinates of the present phosphor as a function of Ce^{3+} concentrations. From the figure, it can be seen very clearly that the coordinates do not vary much with the changing of the Ce^{3+} concentration. The estimated CIE coordinates for the optimized (1 mol% Ce^{3+}- doped CYO) phosphor are ($x = 0.1484$, $y = 0.0987$), which are much closer to the commercial blue phosphor (BAM).

One more important technique to evaluate the practical applicability of a phosphor is CCT (common color temperature), as it specifies the color visuality of the light that is emitted by the light source. The CCT is nothing but the color temperature with respect to the point on the Planckian locus that is nearest to the point representing the chromaticity of the illuminant that is considered on the (u', v') CIE 1976 chromaticity coordinates. The CCT can be calculated by transforming the (x, y) coordinates of the light source to (u', v') using the following well-known equations:

$$u' = \frac{4x}{-2x+12y+3}, \tag{3}$$

$$v' = \frac{9y}{-2x + 12y + 3}, \tag{4}$$

From the McCamy's approximation [33], the CCT value can be calculated from the CIE color coordinates using the third-power polynomial that is given by the following expression:

$$T = -449\,n^3 + 3525\,n^2 - 6823.3\,n + 5520.33, \tag{5}$$

where $n = (x - 0.3320)/(y - 0.1858)$. Table 3 specifies the calculated CCT values for the $CaYAl_3O_7:Ce^{3+}$ phosphors which clearly show their range from 2000 to 3500 K. Generally, CCT values less than 5000 K are considered to produce the warm white light

Table 3
CIE 1931 and 1976 Chromaticity co-ordinates CCT and color purity values of $CaYAl_3O_7:Ce^{3+}$ phosphor.

Phosphors code	CIE 1931 co-ordinates		CIE 1976 co-ordinates		CCT values (K)	Color purity (%)
	x	y	u'	v'		
CY1	0.1484	0.0788	0.1672	0.1944	1972	86.2
CY2	0.1484	0.0987	0.1527	0.2285	2594	90.4
CY3	0.1474	0.0977	0.1521	0.2268	2568	88.3
CY4	0.1469	0.0833	0.1586	0.2023	2049	86.0
CY5	0.1466	0.0994	0.1504	0.2294	2673	90.2
CY6	0.1465	0.1112	0.1450	0.2476	3445	94.7

Table 4
CIE chromaticity coordinate (x, y) and color purity of some important blue light emitting phosphors and the commercial blue emitting BAM:Eu^{2+} phosphor.

Sl. No.	Phosphors	Chromaticity co-ordinates (x, y)	Color purity	Reference
1	$CaYAl_3O_7:Ce^{3+}$	(0.1484, 0.0987)	90.4%	Present work
2	$BAM:Eu^{2+}$	(0.1417, 0.1072)	88.0%	[35]
3	$Sr_2B_2O_5:Tm^{3+}$	(0.1730, 0.1650)	70.0%	[36]
4	$NaBaBO_3:Tm^{3+}$	(0.1470, 0.1090)	86.0%	[37]
5	$KBaBP_2O_8:Tm^{3+}$	(0.1510, 0.0227)	93.3%	[38]
6	$Y_2O_3:Tm^{3+}$	(0.1580, 0.1500)	78.0%	[39]
7	$CaBi_2B_2O_7:Tm^{3+}$	(0.1530, 0.0350)	97.0%	[40]

efficiently that is used in domestic applications [34]. Hence, these materials are precisely applicable for the blue-light production in domestic appliances.

It is well known that the color purity of the phosphors is another key parameter in the evaluation of an enhanced LED light source. For broad- or multiband light sources (white light), the CCT is additionally useful, thereby making the calculation of the color purity of the emitted blue light necessary, and is done by the following formula:

$$Color \quad purity = \frac{\sqrt{(x - x_{ee})^2 + (y - y_{ee})^2}}{\sqrt{(x_d - x_{ee})^2 + (y_d - y_{ee})^2}} \times 100\%, \tag{6}$$

where (x, y), (x_{ee}, y_{ee}), and (x_d, y_d) are the chromaticity coordinates of the sample point, the equal-energy point (0.3333, 0.3333), and the dominant-wavelength point, respectively. The color purity of the $CaYAl_3O_7:Ce^{3+}$ phosphors found to be in the range of 86–94% and which are in the vicinity of the standard blue emitting BAM phosphor. From the results obtained for color-purity (Table 4), it is clear that the phosphor having composition of the $CaYAl_3O_7:Ce^{3+}$ (1 mol%) is the best as it shows the maximum blue emission and an excellent color chromaticity with an improved color purity. Table 4 gives the comparison of the color purity of our present blue-emitting phosphor and commercially available blue-emitting phosphor. Further, it is worth mentioning that the color purity of $CaYAl_3O_7:Ce^{3+}$ is either similar or higher than those of the commercial blue-phosphor $BAM:Eu^{2+}$ and the other blue-light-emitting phosphors. These results justify the potential applicability of $CaYAl_3O_7:Ce^{3+}$ phosphors in solid-state-lighting and optoelectronic-device applications.

4. Conclusions

Solution combustion method was successfully implied to synthesize Blue-light-emitting $CaYAl_3O_7:Ce^{3+}$ phosphors. This method offers a rapid, facile, and morphological uniqueness. XRD results confirmed tetragonal structure of the compounds. The PL-emission spectra displayed a broad emission peak centered at 434 nm that is projecting an intense blue emission. The purity of the blue emission was characterized and the obtained CIE, CCT and color purity results proved the suitability of the present Ce^{3+}-doped CYO as a promising candidate for white-lighting and display device applications.

Acknowledgements

This research was supported by Basic Science Research Program through the National Research Foundation of Korea (NRF) funded by the Ministry of Education (NRF-2016R1D1A1B03932163).

References

[1] G. Li, Y. Zhang, D. Geng, M. Shang, C. Peng, Z. Cheng, J. Lin, Single-composition trichromatic white-emitting $Ca4Y_6(SiO4)_6O:Ce^{3+}/Mn^{2+}/Tb^{3+}$ phosphor: luminescence and energy transfer, ACS Appl. Mater. Interfaces 4 (2012) 296–305.
[2] X.Z. Du, H. Lu, D.J. Chen, X.Q. Xiu, R. Zhang, Y.D. Zheng, UV light-emitting diodes at 340 nm fabricated on a bulk GaN substrate, Chin. Phys. Lett. 27 (2010) 088105-1-088105-3.
[3] L. Shi, Y. Huang, H.J. Seo, Emission red shift and unusual band narrowing of Mn^{2+} in $NaCaPO_4$ phosphor, J. Phys. Chem. A 114 (2010) 6927–6934.
[4] S. Yan, J. Zhang, X. Zhang, S. Lu, X. Ren, Z. Nie, X. Wang, Enhanced red emission in $CaMoO_4:Bi^{3+},Eu^{3+}$, J. Phys. Chem. C 111 (2007) 13256–13260.
[5] T.L. Zhou, Z. Song, X.P. Song, L. Bian, Q.L. Liu, A red oxide phosphor, $Sr_2ScAlO_5:Eu^{2+}$ with perovskite-type structure, for white light-emitting diodes, Chin. Phys. B 19 (2010) 127808-1-127808-4.
[6] Sk.Khaja Hussain, J.S. Yu, Broad red-emission of $Sr_3Y_2Ge_3O_{12}:Eu^{2+}$ garnet phosphors under blue excitation for warm WLED applications, RSC Adv. 7 (2017) 13281–13288.
[7] V. Singh, S. Watanabe, T.K.G. Rao, H.Y. Kwak, Synthesis, characterization, luminescence and defect centres in $CaYAl_3O_7:Eu^{3+}$ red phosphor, J. Flouresc. 21 (2011) 313–320.
[8] V. Singh, V.V.R.K. Kumar, R.P.S. Chakradhar, H.Y. Kwak, Synthesis, characterization and photoluminescence of Eu^{3+}, Ce^{3+} co-doped $CaLaAl_3O_7$ phosphors, Philos. Mag. 90 (2010) 3095–3105.
[9] X. Zhang, J. Zhang, L. Liang, Q. Su, Luminescence of $SrGdGa_3O_7:RE^{3+}$(RE = Eu, Tb) phosphors and energy transfer from Gd^{3+} to RE^{3+}, Mater. Res. Bull. 40 (2005) 281–288.
[10] H.Y. Jiao, Y.H. Wang, A potential red-emitting phosphor $CaSrAl_2SiO_7:Eu^{3+}$ for near-ultraviolet light-emitting diodes, Phys. B 407 (2012) 2729–2733.
[11] H.W. Zhang, H. Yamada, N. Terasaki, C.N. Xu, Blue light emission from stress-activated $CaYAl_3O_7$:Eu, J. Electrochem. Soc. 155 (2008) J128–J131.

[12] H.W. Zhang, C.N. Xu, N. Terasaki, H. Yamada, Electro-mechano-optical luminescence from $CaYAl_3O_7$:Ce, Electrochem. Solid-State Lett. 14 (2011) J76–J80.
[13] A. Bao, C. Tao, H. Yang, Synthesis and luminescent properties of nanoparticles $GdCaAl_3O_7:RE^{3+}$ (RE = Eu, Tb) via the sol-gel method, J. Lumin. 126 (2007) 859–865.
[14] J. Liao, H. You, D. Zhou, H.R. Wen, R. Hong, Sol-gel preparation and photoluminescence properties of $LiLa(MoO_4)_2:Eu^{3+}$ phosphors, Opt. Mater. 34 (2012) 1468–1472.
[15] Y. Hongling, Y. Xue, X. Xuhui, J. Qing, J. Tingming, L. Xuee, Z. Dacheng, J. Qiu, Effects of charge compensation on red emission in $CaYAl_3O_7:Eu^{3+}$ phosphor, Chin. Opt. Lett. 12 (2014) 051602–051604.
[16] Y. Hong-Ling, Y. Xue, X. Xu-Hui, J. Ting-Ming, Y. Peng-Hui, J. Qing, Z. Da-Cheng, Q. Jian-Bei, Characterization and luminescence of Eu/Sm-coactivated $CaYAl_3O_7$ phosphor synthesized by using a combustion method, Chin. Phys. B 22 (2013) 098503-1-098503-4.
[17] P. Halappa, S. Thilak Raj, R. Sairani, S. Joshi, R. Madhusudhana, C. Shivakumara, Combustion synthesis and characterisation of Eu^{3+}-activated Y_2O_3 red nanophosphors for display device applications, Int. J. Nanotechnol. 14 (2017) 833–837.
[18] P. Lecoq, M. Schussler, M. Schneegans, Progress and prospects in the development of new scintillators for future high energy physics experiments, Nucl. Instr. Meth. A 315 (1992) 337–343.
[19] W.G. Lee, D.H. Lee, Y.K. Kim, J.K. Kim, J.W. Park, Growth and characteristics of Gd_2SiO_5 crystal doped Ce^{3+}, J. Nucl. Sci. Technol. 4 (2008) 572–574.
[20] M.D. Dramicanin, V. Jokanovic, E. Antic-Fidancev, M. Mitric, Z. Andric, Luminescence and structural properties of $Gd_2SiO_5:Eu^{3+}$, nanophosphors synthesized from the hydrothermal obtained silica sol, J. Alloys Compd. 424 (2006) 213–217.
[21] R.F. Wei, H. Zhang, F. Li, H. Guo, Blue-white-green tunable luminescence of Ce^{3+}, Tb^{3+} Co-doped sodium silicate glasses for white LEDs, J. Am. Ceram. Soc. 95 (2012) 34–36.
[22] S.H. Park, K.H. Lee, S. Unithrattil, H.S. Yoon, H.G. Jang, W.B. lm, Melilite-structure $CaYAl_3O_7:Eu^{3+}$ phosphor: structural and optical characteristics for near-UV LED-based white light, J. Phys. Chem. C 116 (2012) 26850–26856.
[23] L. Huang, M. Guo, S. Zhao, D. Deng, H. Wang, Y. Hua, G. Jia, S. Xu, Luminescence of $Ca2LiSiO_4F$: Ce^{3+}, Tb^{3+} phosphors, ECS J. Solid State Sci. Technol. 2 (2013) R3083–R3087.
[24] Z.G. Xia, R.S. Lui, Tunable blue-green color emission and energy transfer of $Ca_2Al_3O_6F:Ce^{3+}$,Tb^{3+} phosphors for near-UV white LEDs, J. Phys. Chem. C 116 (2012) 15604–15609.
[25] H. Lin, H. Liang, B. Han, J. Zhong, Q. Su, P. Dorenbos, M.D. Birowosuto, G. Zhang, Y. Fu, W. Wu, Luminescence and site occupancy of Ce^{3+} in $Ba_2Ca(BO_3)_2$, Phys. Rev. B 76 (2007) 035117-1-035117-8.
[26] H. Yu, X. Yu, X. Xu, T. Jiang, P. Yang, Q. Jiao, D. Zhou, J. Qiu, Excitation band extended in $CaYAl_3O_7$: Tb^{3+} phosphor by Ce^{3+} co-doped for NUV light-emitting diodes, Optics Commun. 317 (2014) 78–82.
[27] S. Dutta, S. Som, S.K. Sharma, Luminescence and photometric characterization of K^+ compensated $CaMoO_4:Dy^{3+}$ nanophosphors, Dalton Trans. 42 (2013) 9654–9661.
[28] D.L. Dexter, A theory of sensitized luminescence in solids, J. Chem. Phys. 21 (1953) 836–850.
[29] G. Blasse, Energy transfer between inequivalent Eu^{2+} ions, J. Solid State Chem. 62 (1986) 207–211.
[30] C. Shivakumara, R. Saraf, P. Halappa, White luminescence in Dy^{3+} doped BiOCl phosphors and their Judd-Ofelt analysis, Dyes Pigments 126 (2016) 154–164.
[31] L.G. Van Uitert, Characterization of energy transfer interactions between rare earth ions, J. Electrochem. Soc. 114 (1967) 1048–1053.
[32] P. Halappa, C. Shivakumara, R. Saraf, H. Nagabhushana, Synthesis, structure and photoluminescence properties of Sm^{3+}-doped BiOBr phosphor, AIP Conf. Proc. 1731 (2016) 140064-3.
[33] C.S. McCamy, Correlated color temperature as an explicit function of chromaticity coordinates, Color Res. Appl. 17 (1992) 142–144.
[34] http://www.hunterlab.com/appnotes/an05_05.pdf for specific color index.
[35] W. Liu, C. Huang, C. Wu, Y. Chiu, Y. Yeh, T. Chen, High efficiency and high color purity blue-emitting $NaSrBO_3:Ce^{3+}$ phosphor for near-UV light-emitting diodes, J. Mater. Chem. 21 (2011) 6869–6874.
[36] L. Cai, L. Ying, J. Zheng, B. Fan, R. Chen, C. Chen, Luminescent properties of $Sr_2B_2O_5$: Tm^{3+}, Na^+ blue phosphor, Ceram. Int. 40 (2014) 6913–6918.
[37] J. Zheng, Q. Cheng, L. Ying, L. Cai, C. Chen, Luminescence properties of a novel blue-emitting phosphor $NaBaBO_3:Tm^{3+}$, K^+, Mater. Sci. Forum 833 (2015) 39–43.
[38] B. Han, J. Zhang, P.J. Li, H.Z. Shi, $KBaBP_2O_8:Tm^{3+}$: a novel blue-emitting phosphor with high color purity, JETP Lett. 99 (2014) 561–564.
[39] J.H. Hao, S.A. Studenikin, M. Cocivera, Blue, green and red cathodoluminescence of Y_2O_3 phosphor films prepared by spray pyrolysis, J. Lumin. 93 (2001) 313–319.
[40] J. Li, H. Yan, F. Yan, A novel high color purity blue-emitting phosphor: $CaBi_2B_2O_7:Tm^{3+}$, Mater. Sci. Engg. B 209 (2016) 56–59.